Original Article | Oncologic Imaging

eISSN 2005-8330
https://doi.org/10.3348/kjr.2024.1266
Korean J Radiol 2025;26(6):593-603

Korean Journal of Radiology
KJR

Potential of C-X-C-Chemokine-Receptor-Type-4-Directed PET/CT Using [^{18}F]AlF-NOTA-QHY-04 in Identifying Molecular Subtypes of Small Cell Lung Cancer

Yuxi Luo[1,2]*, Kai Cheng[3]*, Jingru Liu[2,4], Jinli Pei[2], Shengnan Xu[2], Xinzhi Zhao[2], Shijie Wang[2], Kunlong Zhao[2], Wanhu Li[3], Jie Liu[2], Jinming Yu[1,2]

[1]Department of Oncology, The Affiliated Hospital of Southwest Medical University, College of Clinical Medicine, Southwest Medical University, Luzhou, China
[2]Shandong Provincial Key Laboratory of Precision Oncology, Shandong Cancer Hospital and Institute, Shandong First Medical University and Shandong Academy of Medical Sciences, Jinan, China
[3]Department of PET/CT Center, Shandong Cancer Hospital and Institute, Shandong First Medical University and Shandong Academy of Medical Sciences, Jinan, China
[4]Department of Oncology, Renmin Hospital of Wuhan University, Wuhan, China

Objective: Molecular subtyping of small-cell lung cancer (SCLC) has major implications for prognostic relevance and treatment guidance. This study aimed to explore the feasibility of a novel tracer targeting C-X-C-chemokine-receptor-type-4 (CXCR4) for distinguishing different SCLC subtypes.

Materials and Methods: Thirty-five patients with pathologically confirmed SCLC were enrolled in this prospective study. Immunohistochemical staining was performed to classify the molecular subtypes into SCLC-A, SCLC-N, SCLC-P, and SCLC-I. [^{18}F]AlF-NOTA-QHY-04 PET/CT parameters were obtained, including the maximum, mean, and peak standard uptake values (SUV_{max}, SUV_{mean}, and SUV_{peak}, respectively) and the ratios of tumors (T) and normal tissues (NT) based on the SUV_{max} (T/NT). These parameters were compared among the molecular subtypes. A receiver operating characteristic (ROC) curve was used to analyze the performance of the parameters for distinguishing SCLC-N from other subtypes and neuroendocrine (NE) subtypes (SCLC-A and SCLC-N) from non-NE subtypes (SCLC-P and SCLC-I).

Results: The molecular subtypes were SCLC-A (n = 17), SCLC-N (n = 6), SCLC-P (n = 7), and SCLC-I (n = 5). The SCLC-N subtype exhibited significantly higher uptake in both primary tumors and lymph node metastases than the other three subtypes ($P < 0.05$). When SCLC-N was compared with the other three subtypes combined (referred to as "other SCLCs"), all parameters were significantly higher in the SCLC-N group ($P < 0.05$). ROC analysis showed that these parameters had high accuracy in distinguishing SCLC-N from other SCLCs (area under ROC curve: 0.868–0.948 for primary tumors and 0.783–0.888 for lymph node metastases). Compared with the non-NE group, the SUV_{max}, SUV_{mean}, and T/NT_{lung} were significantly higher in the NE group for primary tumors. ROC analysis showed moderate accuracy in distinguishing between the NE and non-NE groups (ROC area: 0.692–0.786 for primary tumors and 0.692–0.815 for lymph node metastases).

Conclusion: Our preliminary findings indicate that CXCR4-directed PET/CT imaging using [^{18}F]AlF-NOTA-QHY-04 may differentiate between SCLC-N and other molecular subtypes and between NE and non-NE subtypes of SCLC.

Keywords: C-X-C motif chemokine receptor 4; PET/CT; Small cell lung cancer; Molecular subtype; Neuroendocrine carcinoma

Received: August 12, 2024 **Revised:** February 24, 2025 **Accepted:** March 6, 2025

*These authors contributed equally to this work.
Corresponding author: Jinming Yu, MD, PhD, Department of Oncology, The Affiliated Hospital of Southwest Medical University, College of Clinical Medicine, Southwest Medical University, No. 1 Section 1, Xiang Lin Road, Longmatan District, Luzhou 646000, China
• E-mail: sdyujinming@163.com
Corresponding author: Jie Liu, MD, Shandong Provincial Key Laboratory of Precision Oncology, Shandong Cancer Hospital and Institute, Shandong First Medical University and Shandong Academy of Medical Sciences, No. 440, Jiyan Road, Huaiyin District, Jinan 250117, China
• E-mail: linchuangliujie@163.com

INTRODUCTION

Small-cell lung cancer (SCLC), which accounts for 15% of all lung cancers, is an exceptionally recalcitrant malignancy with a 5-year survival rate of less than 7% [1,2]. Although molecular typing has improved survival outcomes for patients with various tumor entities, effective molecular subtype classification of SCLC is urgently needed to enhance patient survival [3,4].

Based on the differential expression patterns of transcription factors, SCLC can be stratified into four molecular subsets: SCLC-A (ASCL1-defined), SCLC-N (NEUROD1-defined), SCLC-P (POU2F3-defined), and SCLC-I (inflamed) [5-7]. Typically, SCLC-A and SCLC-N are classified as neuroendocrine (NE) subtypes, whereas SCLC-P and SCLC-I are non-NE [3,8,9]. In different molecular subtypes, distinct expression profiles show potential therapeutic vulnerabilities and different optimal treatment plans must be adopted. For non-NE subtypes, SCLC-I demonstrated the most significant benefit from combined immunotherapy and chemotherapy, while SCLC-P was associated with a good prognosis in surgically resected cases [7,8,10]. Compared to non-NE subtypes, NE phenotypes exhibit greater uncertainty. SCLC-A and SCLC-N are related to the chemosensitivity of SCLC cell lines [7,11]. However, SCLC-N exhibits greater T-cell dysfunction with less immune infiltration [12], leading to lower survival rates in clinical treatment [8]. Therefore, accurate subtype identification is crucial to guide therapy and potentially improve the survival of patients with SCLC.

Currently, SCLC subtyping relies primarily on omics sequencing and immunohistochemistry (IHC). Because surgery is rarely performed for SCLC, patient samples are usually limited to invasive biopsies. Furthermore, tumor heterogeneity presents a significant challenge, underscoring the need for advanced diagnostic methods for SCLC subtyping.

C-X-C chemokine receptor type 4 (CXCR4) is a crucial factor in cell migration and proliferation. Elevated CXCR4 levels correlate with cancer progression, therapy resistance, and poor outcomes in solid tumors, making it a promising target for therapeutic guidance and peptide receptor-based radionuclide therapies [13-15]. In previous studies, we developed a novel ^{18}F-labeled CXCR4-targeting tracer ([^{18}F]AlF-NOTA-QHY-04), which has a more suitable half-life than ^{68}Ga and can be used for detection of SCLC, lymphoma, glioma, and early radiation-induced lung injury [16,17]. Given its imaging capabilities for detecting SCLC, we hypothesized that [^{18}F]AlF-NOTA-QHY-04 PET/CT may be able to distinguish between different SCLC subtypes.

In this prospective study, we aimed to investigate whether the novel tracer [^{18}F]AlF-NOTA-QHY-04 can serve as a non-invasive tool to distinguish different molecular subtypes of SCLC.

MATERIALS AND METHODS

All patients provided informed consent to participate in this study, which was approved by the Institutional Review Board of Shandong Cancer Hospital and Institute (IRB No. SDZLEC2023-256-01).

Study Population

Thirty-five patients with histologically confirmed SCLC were enrolled in this study at the Shandong Cancer Hospital and Institute between January 2023 and September 2024. We acquired the standard uptake values (SUVs) on [^{18}F]AlF-NOTA-QHY-04 PET/CT and biopsy samples from each individual and then conducted IHC staining to classify SCLC subtypes. Finally, the parameters of [^{18}F]AlF-NOTA-QHY-04 were compared among the different subsets.

Patients were enrolled according to the following criteria: 1) age ≥18 years, 2) voluntary participation in the study, and 3) Karnofsky performance status ≥70. The exclusion criteria were as follows: 1) other types of lung tumors, such as large cell lung cancer, adenocarcinoma, squamous cell carcinoma, and adenosquamous carcinoma, 2) administration of any antitumor therapy before the [^{18}F]AlF-NOTA-QHY-04 PET/CT scan, and 3) history of allergy to the radiotracer.

A flowchart of the study is shown in Figure 1. Thirty-five patients with SCLC were randomly recruited for analysis. This study complied with the updated Declaration of Helsinki guidelines (unproven clinical practice interventions).

Molecular Subtyping Based on IHC

Conventional IHC staining of ASCL1 (Clone: 24B72D11.1, Cat# 556604, BD Biosciences, 1:25), NEUROD1 (Clone: EPR20766, Cat# ab213725, Abcam, 1:1000), and POU2F3 (Clone: polyclonal, Cat# NBP1-83966, Novus Biologicals, 1:200) was performed on formalin-fixed paraffin-embedded tissue sections (4–5 μm) prepared from the biopsy samples of the 35 patients in Shandong Cancer Hospital and Institute. Tumor cells with DAB-stained nuclei were

https://doi.org/10.3348/kjr.2024.1266

Korean Journal of Radiology
KJR

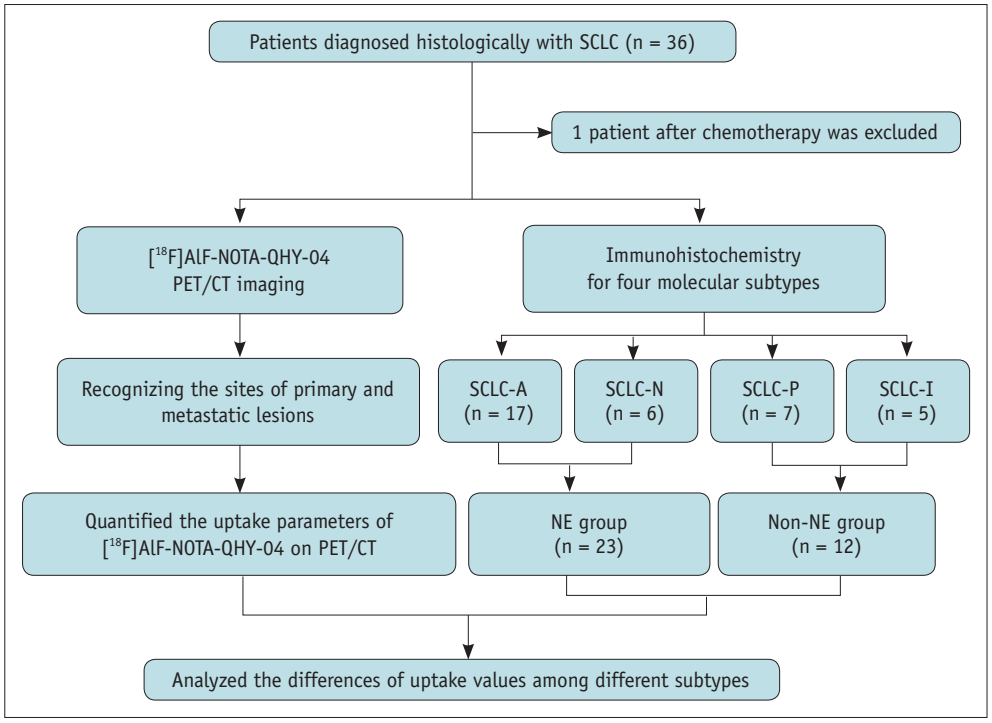

Fig. 1. Study flowchart. SCLC = small-cell lung cancer, NE = neuroendocrine

considered positive, and a histoscore (H-score) system was applied by multiplying the percentage of positive tumor cells (1%–100%) by the staining intensity (1 = weak, 2 = moderate, and 3 = strong) in tumor cells [18-20].

To describe these subtype markers, H-scores >10 were considered positive [21]. Notably, if multiple markers had H-scores >10, the most prominent expression of these markers was defined as the marker with the highest H-score. Two pathologists used a multi-headed microscope and discussed each slide of the IHC results.

[^{18}F]AlF-NOTA-QHY-04 PET/CT Scanning

[^{18}F]AlF-NOTA-QHY-04 was synthesized and administered as previously described [17]. Blood glucose measurements and fasting were not performed prior to the examination. Patients underwent CXCR4-directed PET/CT 60 minutes after intravenous injection of 4.81 MBq/kg of [^{18}F]AlF-NOTA-QHY-04.

The follow-up PET/CT scans were performed on an integrated in-line PET/CT system (GEMINI TF Big Bore; Philips Healthcare, Cleveland, OH, USA). Fused PET/CT images of coronal, sagittal, and transaxial slices were viewed on a Xeleris workstation (GE HealthCare, Waukesha, WI, USA). Regular breathing was allowed during the image acquisition period.

Image Analysis

All [^{18}F]AlF-NOTA-QHY-04 PET/CT scans were collaboratively analyzed visually by two board-certified nuclear medicine physicians with more than 20 years of experience. Additional imaging modalities, including contrast-enhanced CT, MRI, and PET-CT, were also utilized and assessed by a multidisciplinary team of radiologists and oncologists. After a comprehensive evaluation of both primary and metastatic lesions using these imaging techniques, the team reached a consensus on the diagnosis and staging. In our study, we used a semi-automatic contour segmentation method, setting the threshold at 42% of the tumor maximum standardized uptake value (SUV_{max}) to determine the three-dimensional volumes of regions of interest (ROIs). To ensure accuracy, all segmentation results were reviewed by nuclear medicine physicians and ambiguous cases were resolved by consensus. SUVs were calculated by multiplying the measured activity concentration (Bq/mL) and body weight (g) by injected activity (Bq). The primary tumor and metastatic site uptake intensities were recorded, including SUV_{max}, mean standardized uptake value (SUV_{mean}), and peak standardized uptake value (SUV_{peak}). Here, we primarily evaluated lymph node metastasis using a comprehensive approach that incorporated PET/CT parameters, anatomical distribution,

 https://doi.org/10.3348/kjr.2024.1266

morphological features, and enhancement patterns to determine whether the lymph nodes were metastatic. The background activity of healthy lungs was outlined to obtain the SUV_{max}. The SUV_{max} of the blood pool was measured by placing a 15-mm ROI in the center of the right atrium (L2-L4). The tumor-to-normal ratios of tracer uptake based on SUV_{max} were calculated and denoted as T/NT_{lung} and T/NT_{blood} [22].

Statistical Analysis

Data for SUV_{max}, SUV_{mean}, SUV_{peak}, T/NT_{blood}, and T/NT_{lung} are expressed as mean ± standard deviation. Statistical tests were performed with SPSS (version 17.0, SPSS Inc., Chicago, IL, USA). GraphPad Prism (version 8.0.2, GraphPad Software, San Diego, CA, USA) was used for data visualization and statistical analyses.

One-way ANOVA was used to compare PET/CT uptake values among the four molecular subtypes. Following a significant one-way ANOVA result, post-hoc pairwise comparisons were conducted using Tukey's HSD test. Based on the results of the normality tests, either two-sample *t*-tests or Mann-Whitney U tests were used to compare differences in PET/CT parameters between the two groups. Receiver operating characteristic (ROC) analysis was used to evaluate the diagnostic performance of these imaging parameters in distinguishing between SCLC-N and other types combined and between the NE and non-NE groups. Statistical significance was set at $P < 0.05$, and all *P*-values were two-tailed.

RESULTS

Characteristics of the Enrolled Patients

Thirty-five patients (26 male and 9 female) were enrolled in the study. The median age of the patients was 67 years (range: 38–80 years), and 21 patients were diagnosed with extended disease, with 14 individuals having limited stages. The demographic characteristics and clinical information of the patients are summarized in Table 1. Based on the IHC expression of ASCL1, NEUROD1, and POU2F3, SCLC were categorized into different molecular subtypes. We found that SCLC-A was the dominant subtype and was observed in 48.6% (17/35) of patients, followed by SCLC-P, SCLC-N, and SCLC-I in 20.0% (7/35), 17.1% (6/35), and 14.3% (5/35) of patients, respectively (Fig. 2).

Table 1. Characteristics of the SCLC patients (n = 35)

Characteristic	Value
Age, yrs, median (range)	67 (38–80)
Sex	
Male	26 (74.3)
Female	9 (25.7)
Molecular subtype	
SCLC-A	17 (48.6)
SCLC-N	6 (17.1)
SCLC-P	7 (20.0)
SCLC-I	5 (14.3)
Stage	
Limited stage	14 (40.0)
Extensive stage	21 (60.0)
TNM classification	
I	1 (2.9)
II	1 (2.9)
III	12 (34.2)
IV	21 (60.0)
Karnofsky performance status	
80	21 (60.0)
90	14 (40.0)

Data are number of patients with percentage in parentheses, unless specified otherwise.
SCLC = small-cell lung cancer, TNM = tumor node metastasis

Comparison of [^{18}F]AlF-NOTA-QHY-04 Parameters Between Different Molecular Subtypes

Quantitative parameters, including SUV_{max}, SUV_{mean}, SUV_{peak}, T/NT_{blood}, and T/NT_{lung} of the primary lesions and lymph node metastases, are shown in Table 2. In the primary lesion, SUV_{max}, SUV_{mean}, SUV_{peak}, T/NT_{blood}, and T/NT_{lung} were all higher in SCLC-N than in the other three subtypes (all $P < 0.05$, Fig. 3A-E). The uptake values of these five parameters were also higher in SCLC-N than in the other three subtypes for lymph node metastases (all $P < 0.05$, Fig. 3F-J). Intriguingly, the T/NT_{lung} of SCLC-A was higher than that of SCLC-I for lymph node metastases ($P = 0.011$; Fig. 3J).

When comparing SCLC-N with the other SCLCs types combined (SCLC-A, SCLC-P, and SCLC-I), all five parameters were significantly higher in SCLC-N, both in primary lesions and lymph node metastases (all $P < 0.05$; Fig. 3K-T). Representative [^{18}F]AlF-NOTA-QHY-04 PET/CT images of patients with different SCLC molecular subtypes are shown in Figure 4.

The tracer uptake of primary lesions were significantly higher in the NE group than that in the non-NE group, including SUV_{max} (8.08 ± 2.83 vs. 6.22 ± 1.69, $P = 0.045$, Fig. 5A), SUV_{mean} (3.83 ± 1.41 vs. 2.92 ± 0.70, $P = 0.046$, Fig. 5B), and T/NT_{lung} (13.76 ± 5.34, 9.26 ± 1.74, $P = 0.008$,

https://doi.org/10.3348/kjr.2024.1266

Korean Journal of Radiology
KJR

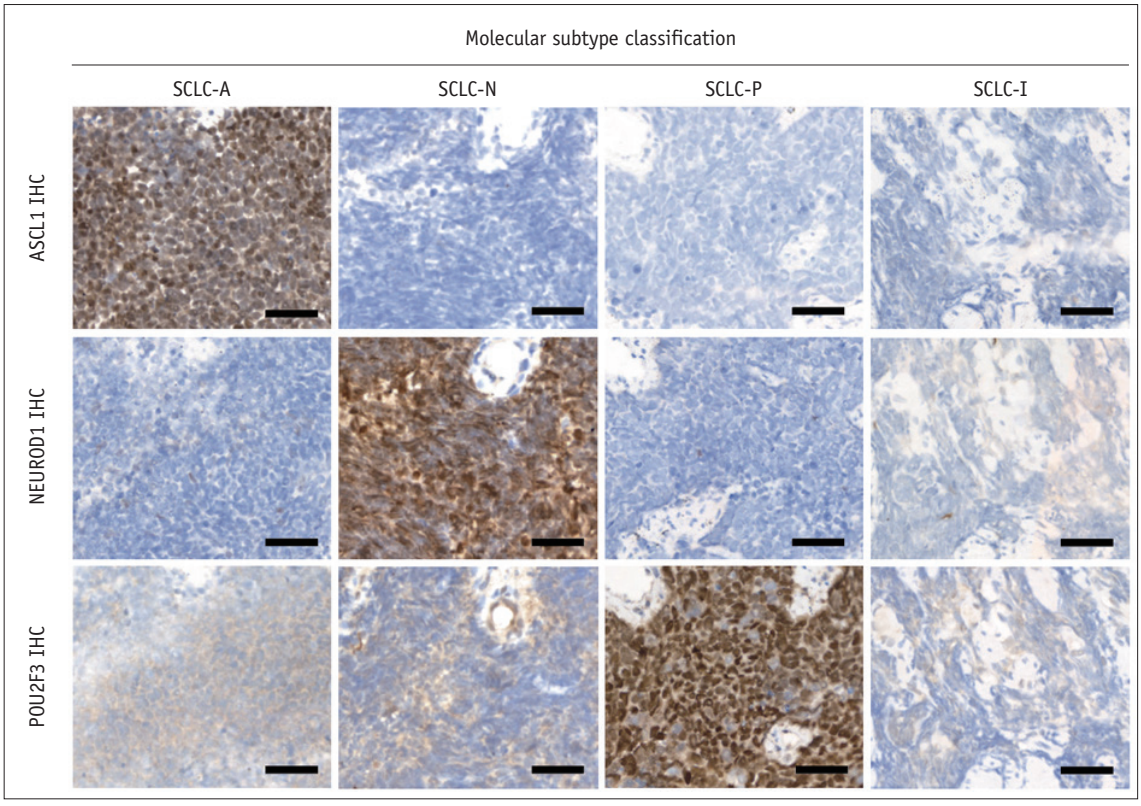

Fig. 2. Representative images of different molecular subtypes in SCLC defined by IHC staining (scale bar: 40 μm). SCLC = small-cell lung cancer, ASCL1 = achaete-scute homolog 1, IHC = immunohistochemistry, NEUROD1 = neurogenic differentiation factor 1, POU2F3 = POU class 2 homeobox 3

Table 2. [^{18}F]AlF-NOTA-QHY-04 PET/CT parameters of primary and metastatic lesions in different molecular types

Parameters	All patients	SCLC-A	SCLC-N	SCLC-P	SCLC-I
Primary lesions					
SUV_{max}	7.44 ± 2.63	7.14 ± 2.54	10.72 ± 1.80	6.16 ± 2.21	6.29 ± 0.73
SUV_{mean}	3.52 ± 1.28	3.39 ± 1.17	5.21 ± 1.07	2.88 ± 0.88	2.99 ± 0.43
SUV_{peak}	5.69 ± 2.20	5.38 ± 2.12	8.31 ± 2.03	4.70 ± 1.78	4.95 ± 0.57
T/NT_{blood}	4.16 ± 1.59	3.83 ± 1.14	6.48 ± 1.84	3.32 ± 1.04	3.67 ± 0.58
T/NT_{lung}	12.22 ± 4.91	12.14 ± 4.25	18.36 ± 5.78	9.85 ± 2.00	8.43 ± 0.91
Lymph node metastases					
SUV_{max}	6.41 ± 1.98	6.19 ± 1.76	8.27 ± 2.05	6.03 ± 1.47	4.95 ± 0.95
SUV_{mean}	3.16 ± 1.13	2.98 ± 0.89	4.39 ± 1.30	2.70 ± 0.47	2.45 ± 0.53
SUV_{peak}	4.64 ± 1.64	4.47 ± 1.37	6.04 ± 1.92	4.29 ± 1.50	3.62 ± 0.83
T/NT_{blood}	3.63 ± 1.48	3.28 ± 1.08	5.30 ± 1.76	3.18 ± 0.84	2.77 ± 0.55
T/NT_{lung}	10.29 ± 3.75	10.37 ± 3.86	14.05 ± 2.30	8.77 ± 2.05	6.91 ± 1.33

Data are mean ± standard deviation.
SCLC = small-cell lung cancer, SUV_{max} = maximum standard uptake value, SUV_{mean} = mean standard uptake value, SUV_{peak} = peak standard uptake value, T/NT_{blood} = ratio of SUV_{max} of the primary tumor to normal tissue (blood pool), T/NT_{lung} = ratio of SUV_{max} of the primary tumor to normal tissue (lung)

Fig. 5E), whereas SUV_{peak} (6.14 ± 2.43 vs. 4.81 ± 1.36, P = 0.088, Fig. 5C) and T/NT_{blood} (4.52 ± 1.77 vs. 3.47 ± 0.87, P = 0.061, Fig. 5D) were not significantly different. For lymph node metastases, all measured parameters were significantly higher in the NE group than in the non-NE group (Fig. 5F-J).

Distinguishing SCLC-N From Other Subgroups and NE Subtypes From Non-NE Subtypes

The diagnostic performance results are summarized in Tables 3-6. ROC analysis revealed that all five parameters had fairly high performance in differentiating SCLC-N from

https://doi.org/10.3348/kjr.2024.1266

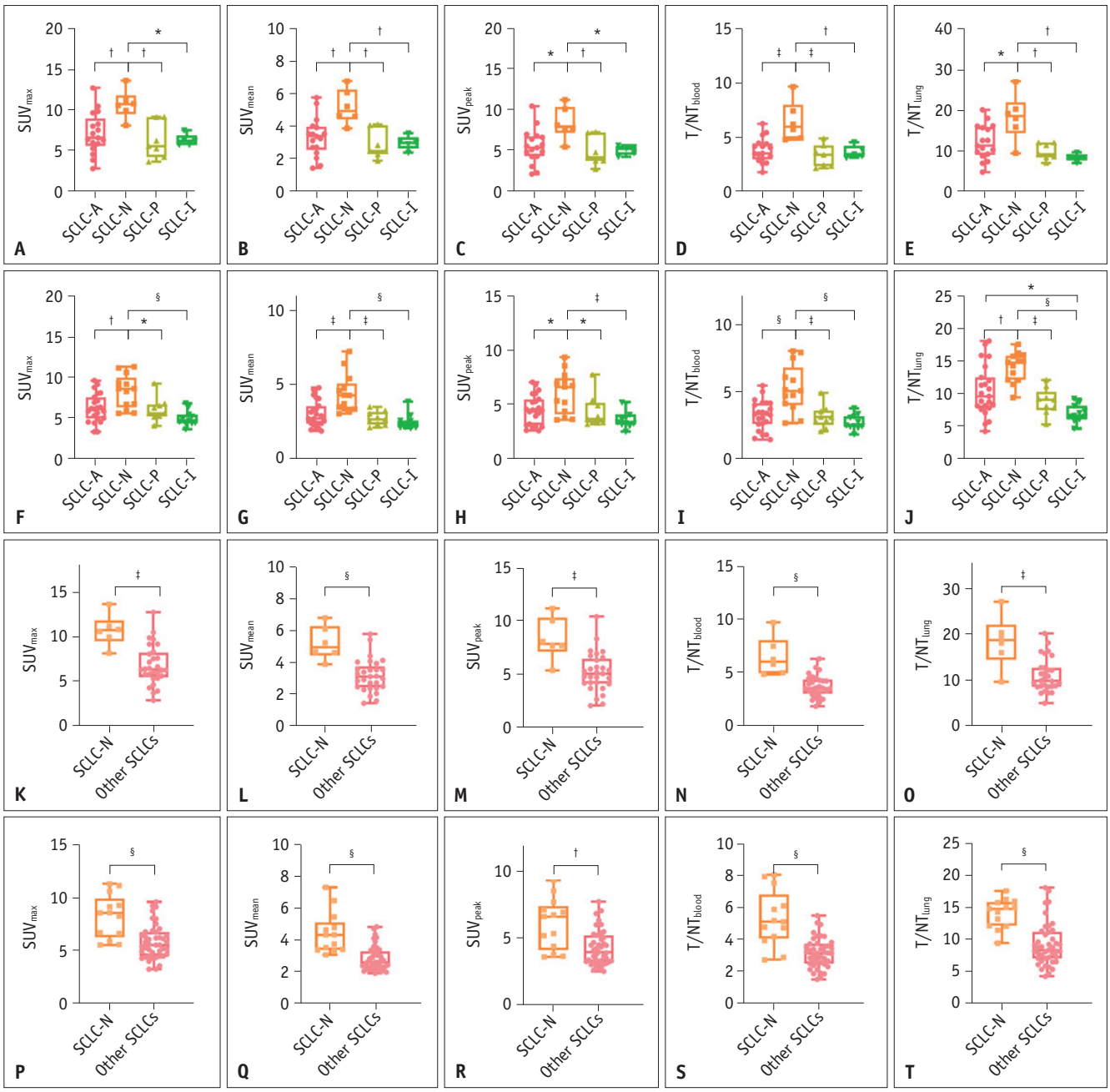

Fig. 3. [^{18}F]AlF-NOTA-QHY-04 PET/CT uptake observed in primary lesions of various molecular subtypes **(A-E, K-O)** and lymph node metastases **(F-J, P-T)**. *P < 0.05, †P < 0.01, ‡P < 0.001, §P < 0.0001. SCLC = small-cell lung cancer, SUV_{max} = maximum standard uptake value, SUV_{mean} = mean standard uptake value, SUV_{peak} = peak standard uptake value, T/NT_{blood} = ratio of SUV_{max} of the primary tumor to normal tissue (blood pool), and T/NT_{lung} = ratio of SUV_{max} of the primary tumor to normal tissue (lung)

other types in both primary lesions (area under the curve [AUC]: 0.868–0.948) and lymph node metastases (AUC: 0.783–0.888) (Tables 3, 4). Among these, T/NT_{blood} was notable with the highest diagnostic performance (AUC: 0.948) with 100.0% sensitivity and 86.2% specificity. Regarding the distinction between the NE and non-NE groups, all parameters showed moderate overall performance for both primary lesions (AUC: 0.692–0.786) and lymph node metastases (AUC: 0.692–0.815) (Tables 5, 6).

DISCUSSION

Our study explored the application of CXCR4-targeted PET/CT imaging to identify the different molecular subtypes

https://doi.org/10.3348/kjr.2024.1266

Korean Journal of Radiology
KJR

of SCLC. We observed a significantly higher uptake in the SCLC-N subtype in both primary tumors and lymph node metastases than in the other subtypes ($P < 0.05$). Notably, the T/NT_{blood} parameter demonstrated the highest diagnostic value for distinguishing SCLC-N from other SCLC subtypes, with an AUC of 0.948, sensitivity of 100%, and specificity

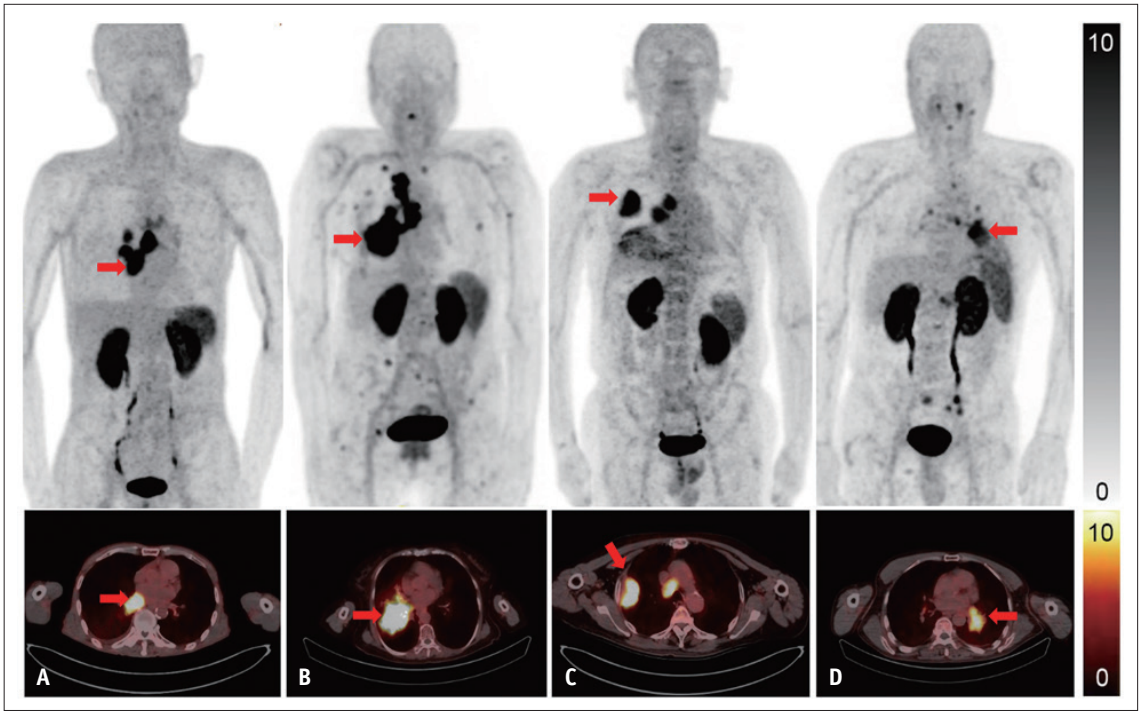

Fig. 4. Representative [^{18}F]AlF-NOTA-QHY-04 PET/CT images of patients with SCLC-A. Primary tumors are indicated by red arrows. **A:** SCLC-A (SUV_{max} = 8.03), **B:** SCLC-N (SUV_{max} = 11.19), **C:** SCLC-P (SUV_{max} = 9.14), **D:** SCLC-I (SUV_{max} = 6.21). SCLC = small-cell lung cancer, SUV_{max} = maximum standard uptake value

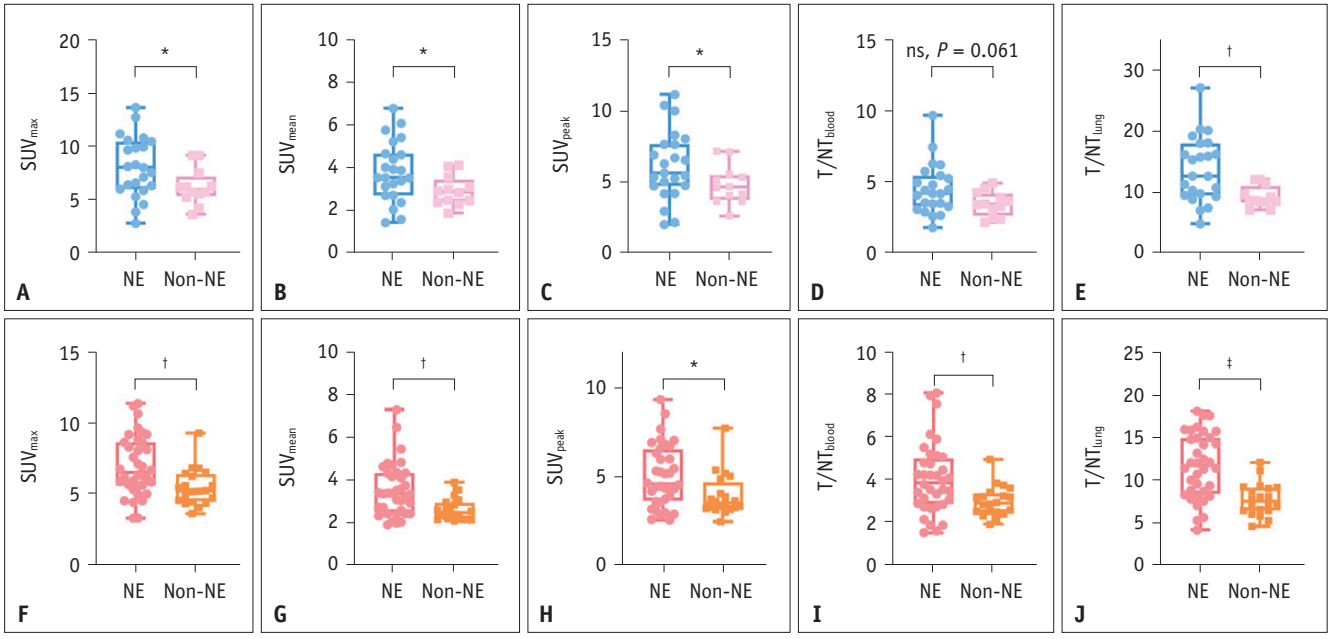

Fig. 5. Comparison between NE and non-NE subtypes based on [^{18}F]AlF-NOTA-QHY-04 PET/CT uptake in primary lesions **(A-E)** and lymph node metastases **(F-J)**. *$P < 0.05$, †$P < 0.01$, ‡$P < 0.0001$. NE = neuroendocrine, SCLC = small-cell lung cancer, SUV_{max} = maximum standard uptake value, SUV_{mean} = mean standard uptake value, SUV_{peak} = peak standard uptake value, ns = not significant, T/NT_{blood} = ratio of SUV_{max} of the primary tumor to normal tissue (blood pool), T/NT_{lung} = ratio of SUV_{max} of the primary tumor to normal tissue (lung)

https://doi.org/10.3348/kjr.2024.1266

Table 3. Performance of [^{18}F]AlF-NOTA-QHY-04 PET/CT parameters for distinguishing SCLC-N and the other SCLCs in primary lesions

Parameters	AUC	Sensitivity, %	Specificity, %	Accuracy, %	Threshold
SUV_{max}	0.931	83.3 (5/6)	93.1 (27/29)	91.4 (32/35)	9.86
SUV_{mean}	0.925	83.3 (5/6)	93.1 (27/29)	91.4 (32/35)	4.40
SUV_{peak}	0.897	83.3 (5/6)	93.1 (27/29)	91.4 (32/35)	7.17
T/NT_{blood}	0.948	100 (6/6)	86.2 (25/29)	88.6 (31/35)	4.57
T/NT_{lung}	0.868	83.3 (5/6)	86.2 (25/29)	85.7 (30/35)	15.75

SCLC = small-cell lung cancer, AUC = area under the curve, SUV_{max} = maximum standard uptake value, SUV_{mean} = mean standard uptake value, SUV_{peak} = peak standard uptake value, T/NT_{blood} = ratio of SUV_{max} of the primary tumor to normal tissue (blood pool), T/NT_{lung} = ratio of SUV_{max} of the primary tumor to normal tissue (lung)

Table 4. Performance of [^{18}F]AlF-NOTA-QHY-04 PET/CT parameters for distinguishing SCLC-N and the other SCLCs in lymph node metastases

Parameters	AUC	Sensitivity, %	Specificity, %	Accuracy, %	Threshold
SUV_{max}	0.825	61.5 (8/13)	90.7 (39/43)	83.9 (47/56)	8.09
SUV_{mean}	0.888	100 (13/13)	69.8 (30/43)	76.8 (43/56)	2.99
SUV_{peak}	0.783	53.9 (7/13)	93.0 (40/43)	83.9 (47/56)	6.31
T/NT_{blood}	0.864	84.6 (11/13)	81.4 (35/43)	82.1 (46/56)	3.80
T/NT_{lung}	0.880	92.3 (12/13)	79.1 (34/43)	82.1 (46/56)	11.28

SCLC = small-cell lung cancer, AUC = area under the curve, SUV_{max} = maximum standard uptake value, SUV_{mean} = mean standard uptake value, SUV_{peak} = peak standard uptake value, T/NT_{blood} = ratio of SUV_{max} of the primary tumor to normal tissue (blood pool), T/NT_{lung} = ratio of SUV_{max} of the primary tumor to normal tissue (lung)

Table 5. Performance of [^{18}F]AlF-NOTA-QHY-04 PET/CT parameters for distinguishing SCLC of NE and non-NE subtypes in primary lesions

Parameters	AUC	Sensitivity, %	Specificity, %	Accuracy, %	Threshold
SUV_{max}	0.732	73.9 (17/23)	75.0 (9/12)	74.3 (26/35)	6.28
SUV_{mean}	0.699	73.9 (17/23)	75.0 (9/12)	74.3 (26/35)	3.10
SUV_{peak}	0.696	78.3 (18/23)	58.3 (7/12)	71.4 (25/35)	4.68
T/NT_{blood}	0.692	60.9 (14/23)	75.0 (9/12)	65.7 (23/35)	3.91
T/NT_{lung}	0.786	56.5 (13/23)	100 (12/12)	71.4 (25/35)	12.09

SCLC = small-cell lung cancer, NE = neuroendocrine, AUC = area under the curve, SUV_{max} = maximum standard uptake value, SUV_{mean} = mean standard uptake value, SUV_{peak} = peak standard uptake value, T/NT_{blood} = ratio of SUV_{max} of the primary tumor to normal tissue (blood pool), T/NT_{lung} = ratio of SUV_{max} of the primary tumor to normal tissue (lung)

Table 6. Performance of [^{18}F]AlF-NOTA-QHY-04 PET/CT parameters for distinguishing SCLC of NE and non-NE subtypes in lymph node metastases

Parameters	AUC	Sensitivity, %	Specificity, %	Accuracy, %	Threshold
SUV_{max}	0.729	75.0 (27/36)	70.0 (14/20)	73.2 (41/56)	5.56
SUV_{mean}	0.747	55.6 (20/36)	90.0 (18/20)	67.9 (38/56)	3.23
SUV_{peak}	0.692	69.4 (25/36)	75.0 (15/20)	71.4 (40/56)	4.03
T/NT_{blood}	0.714	50.0 (18/36)	95.0 (19/20)	66.1 (37/56)	3.80
T/NT_{lung}	0.815	69.4 (25/36)	90.0 (18/20)	76.8 (43/56)	9.35

SCLC = small-cell lung cancer, NE = neuroendocrine, AUC = area under the curve, SUV_{max} = maximum standard uptake value, SUV_{mean} = mean standard uptake value, SUV_{peak} = peak standard uptake value, T/NT_{blood} = ratio of SUV_{max} of the primary tumor to normal tissue (blood pool), T/NT_{lung} = ratio of SUV_{max} of the primary tumor to normal tissue (lung)

of 86.2%. We also validated the performance of PET/CT parameters in distinguishing between the NE and non-NE subtypes. These findings highlight the potential of CXCR4-directed PET/CT as a non-invasive tool for molecular subtyping of SCLC, which could have significant implications for personalized treatment planning.

The elevated tracer uptake in SCLC-N aligns with its distinct biological features. NEUROD1, the defining transcription factor of SCLC-N, is associated with an immune-cold status and promotes tumor cell survival, proliferation, and migration through the regulation of TRKB and NCAM1 [11,23]. These pathways enhance the invasive behavior of NE lung carcinomas [24,25]. High CXCR4 expression, reflected by increased tracer uptake, may be

https://doi.org/10.3348/kjr.2024.1266

Korean Journal of Radiology
KJR

associated with these aggressive features and could explain the poor prognosis often observed in patients with SCLC-N. Similarly, as the most common subtype, SCLC-A showed a relatively high tracer uptake in our study. Similar to SCLC-N, it is considered an immunologically cold tumor [26]. ASCL1 is a key transcription factor that activates NE genes and contributes to cell proliferation [27]. The similar PET/CT characteristics observed between SCLC-A and SCLC-N may reflect their shared NE nature and potentially comparable CXCR4 expression patterns.

In contrast, the non-NE subtypes SCLC-P and SCLC-I displayed reduced CXCR4-directed tracer uptake. SCLC-P, defined by the POU2F3 transcription factor, is characterized by a low expression of NE markers and is associated with a more favorable prognosis [8,21,28]. This may explain the lower CXCR4-directed tracer uptake observed in this subtype. SCLC-I is distinguished by high levels of immune cell infiltration and the expression of immune checkpoint-related genes, which are clinically significant and suggest a stronger response to immunotherapy. In the Phase 3 Impower133 trial, patients with SCLC-I receiving atezolizumab plus chemotherapy showed an 8-month increase in the median overall survival than those receiving chemotherapy alone [7].

The differential tracer uptake among these subtypes may reflect the underlying differences in tumor biology, immune microenvironment, and potential treatment responses. Our ROC analysis demonstrated high sensitivity and specificity for distinguishing SCLC-N from other SCLCs, particularly using the T/NT_{blood} parameter. This suggests that CXCR4-directed PET/CT could serve as a valuable non-invasive tool for identifying SCLC-N subtypes, which may have important implications for prognosis and treatment planning.

Furthermore, the observation of higher tracer uptake in NE than in non-NE subtypes in primary tumors is particularly intriguing. This finding is consistent with previous reports of higher CXCR4 expression in NE SCLC cell lines [29-31]. The ability to non-invasively distinguish NE from non-NE SCLC could have significant clinical implications, as these groups exhibit different immune profiles and treatment responses. Non-NE subtypes, particularly SCLC-I, show better responses to immunotherapy [32-34]. Our imaging approach can potentially help identify patients who are more likely to benefit from immune checkpoint inhibitors.

From a molecular perspective, the association between CXCR4 expression and SCLC subtypes may be explained by shared signaling pathways. For instance, the Wnt signaling pathway, which induces cell migration and proliferation in NE neoplasms, could be activated by CXCR4/CXCL12 [35-38]. Notably, NEUROD1 is also a target of Wnt/β-catenin signaling, which may suggest the potential connection between NEUROD1 and CXCR4/CXCL12. This could partly explain the high uptake of CXCR4-directed tracers observed in SCLC-N. In terms of the tumor microenvironment, higher CXCR4 expression in NE subtypes, particularly SCLC-N, may contribute to their immune-cold phenotype. CXCR4/CXCL12 signaling promotes the exit of $CD8^+$ T cells from the tumor microenvironment [39], potentially explaining the lower immune cell infiltration observed in these subtypes. Conversely, lower CXCR4 expression in non-NE subtypes, especially SCLC-I, may contribute to their immune-hot status and a better response to immunotherapy.

Our findings suggest that [^{18}F]AlF-NOTA-QHY-04 PET/CT imaging may serve as a valuable tool for non-invasive SCLC subtyping, potentially guiding treatment decisions. For instance, patients with lower tracer uptake, which is indicative of non-NE subtypes, may be prime candidates for immunotherapy, whereas those with higher uptake may benefit more from chemotherapy or targeted approaches. The ability to non-invasively assess SCLC subtypes could be particularly valuable given the challenges of obtaining repeated biopsies in patients with SCLC.

However, this study has several limitations. First, our sample size was relatively small and was derived from a single institution, which might limit the generalizability of our findings. Therefore, larger multicenter studies are required to validate these findings. Second, owing to the small sample size, this study was unable to include and analyze various metastatic sites beyond the lymph nodes, as there were insufficient metastatic lesions to allow meaningful analysis. Third, we relied on biopsy specimens for immunohistochemical subtyping, which may not have fully captured tumor heterogeneity. Future studies comparing PET/CT results with those of more comprehensive genomic profiling could provide additional insights.

In conclusion, our results demonstrate that [^{18}F]AlF-NOTA-QHY-04 PET/CT imaging can identify SCLC molecular subtypes, particularly in distinguishing between SCLC-N and other SCLC subtypes, and between NE and non-NE subtypes. The parameters showed relatively high diagnostic performance, particularly the T/N_{blood} in differentiating SCLC-N from other SCLC subtypes. This non-invasive approach could complement existing diagnostic methods and guide individualized treatment strategies.

 https://doi.org/10.3348/kjr.2024.1266

Availability of Data and Material

The datasets generated or analyzed during the study are available from the corresponding author on reasonable request.

Conflicts of Interest

The authors have no potential conflicts of interest to disclose.

Author Contributions

Conceptualization: Jie Liu, Jinming Yu. Data curation: Yuxi Luo, Kai Cheng. Formal analysis: Yuxi Luo, Kai Cheng. Funding acquisition: Shengnan Xu, Jie Liu, Jinming Yu. Investigation: Yuxi Luo, Jingru Liu. Methodology: Jinli Pei, Shijie Wang. Project administration: Jie Liu, Jinming Yu. Resources: Kunlong Zhao, Wanhu Li. Software: Yuxi Luo, Kai Cheng. Supervision: Jie Liu, Jinming Yu. Validation: Yuxi Luo, Jingru Liu. Visualization: Yuxi Luo, Kai Cheng. Writing—original draft: Yuxi Luo. Writing—review, editing: Yuxi Luo, Jingru Liu.

ORCID IDs

Yuxi Luo
https://orcid.org/0000-0003-0412-2307
Kai Cheng
https://orcid.org/0000-0001-9572-9360
Jie Liu
https://orcid.org/0000-0003-2931-2756
Jinming Yu
https://orcid.org/0000-0001-7710-5466

Funding Statement

This work was funded by the foundation of the Research Unit of Radiation Oncology, Chinese Academy of Medical Sciences (2019RU071), the foundation of National Natural Science Foundation of China (81627901, 82203014, 22307068, 82172676, 82030082, and 8203000516), the foundation of Natural Science Foundation of Shandong (ZR2023ZD26, ZR2022QH017, ZR2022QB015, ZR2021YQ52 and ZR2020LZL016), Taishan Scholars Program (NO. tsqn202306386), China Postdoctoral Science Foundation (2023M742149), the Youth Foundation Cultivation Project of Shandong First Medical University (202201–113), and the Shandong Province Traditional Chinese Medicine Science and Technology Project (2021Q002).

REFERENCES

1. Gazdar AF, Bunn PA, Minna JD. Small-cell lung cancer: what we know, what we need to know and the path forward. *Nat Rev Cancer* 2017;17:725-737
2. Schwendenwein A, Megyesfalvi Z, Barany N, Valko Z, Bugyik E, Lang C, et al. Molecular profiles of small cell lung cancer subtypes: therapeutic implications. *Mol Ther Oncolytics* 2021;20:470-483
3. Olbrecht S, Busschaert P, Qian J, Vanderstichele A, Loverix L, Van Gorp T, et al. High-grade serous tubo-ovarian cancer refined with single-cell RNA sequencing: specific cell subtypes influence survival and determine molecular subtype classification. *Genome Med* 2021;13:111
4. Cristescu R, Lee J, Nebozhyn M, Kim KM, Ting JC, Wong SS, et al. Molecular analysis of gastric cancer identifies subtypes associated with distinct clinical outcomes. *Nat Med* 2015;21:449-456
5. Rudin CM, Poirier JT, Byers LA, Dive C, Dowlati A, George J, et al. Molecular subtypes of small cell lung cancer: a synthesis of human and mouse model data. *Nat Rev Cancer* 2019;19:289-297
6. Baine MK, Hsieh MS, Lai WV, Egger JV, Jungbluth AA, Daneshbod Y, et al. SCLC subtypes defined by ASCL1, NEUROD1, POU2F3, and YAP1: a comprehensive immunohistochemical and histopathologic characterization. *J Thorac Oncol* 2020;15:1823-1835
7. Gay CM, Stewart CA, Park EM, Diao L, Groves SM, Heeke S, et al. Patterns of transcription factor programs and immune pathway activation define four major subtypes of SCLC with distinct therapeutic vulnerabilities. *Cancer Cell* 2021;39:346-360.e7
8. Megyesfalvi Z, Barany N, Lantos A, Valko Z, Pipek O, Lang C, et al. Expression patterns and prognostic relevance of subtype-specific transcription factors in surgically resected small-cell lung cancer: an international multicenter study. *J Pathol* 2022;257:674-686
9. Solta A, Ernhofer B, Boettiger K, Megyesfalvi Z, Heeke S, Hoda MA, et al. Small cells - big issues: biological implications and preclinical advancements in small cell lung cancer. *Mol Cancer* 2024;23:41
10. Liu SV, Mok TSK, Nabet BY, Mansfield AS, De Boer R, Losonczy G, et al. Clinical and molecular characterization of long-term survivors with extensive-stage small cell lung cancer treated with first-line atezolizumab plus carboplatin and etoposide. *Lung Cancer* 2023;186:107418
11. Ito T, Kudoh S, Fujino K, Sanada M, Tenjin Y, Saito H, et al. Pulmonary neuroendocrine cells and small cell lung carcinoma: immunohistochemical study focusing on mechanisms of neuroendocrine differentiation. *Acta Histochem Cytochem* 2022;55:75-83
12. Chan JM, Quintanal-Villalonga Á, Gao VR, Xie Y, Allaj V, Chaudhary O, et al. Signatures of plasticity, metastasis, and immunosuppression in an atlas of human small cell lung cancer. *Cancer Cell* 2021;39:1479-1496.e18

13. Nengroo MA, Khan MA, Verma A, Datta D. Demystifying the CXCR4 conundrum in cancer biology: beyond the surface signaling paradigm. *Biochim Biophys Acta Rev Cancer* 2022;1877:188790
14. Bao S, Darvishi M, H Amin A, Al-Haideri MT, Patra I, Kashikova K, et al. CXC chemokine receptor 4 (CXCR4) blockade in cancer treatment. *J Cancer Res Clin Oncol* 2023;149:7945-7968
15. Buck AK, Serfling SE, Lindner T, Hänscheid H, Schirbel A, Hahner S, et al. CXCR4-targeted theranostics in oncology. *Eur J Nucl Med Mol Imaging* 2022;49:4133-4144
16. Cheng K, Wang S, Liu T, Pei J, Wang S, Liu J, et al. PET imaging of CXCR4 expression using [^{18}F]AlF-NOTA-QHY-04 for hematologic malignancy and solid tumors. *Theranostics* 2024;14:6337-6349
17. Pei J, Cheng K, Liu T, Gao M, Wang S, Xu S, et al. Early, non-invasive detection of radiation-induced lung injury using PET/CT by targeting CXCR4. *Eur J Nucl Med Mol Imaging* 2024;51:1109-1120
18. Fedchenko N, Reifenrath J. Different approaches for interpretation and reporting of immunohistochemistry analysis results in the bone tissue - a review. *Diagn Pathol* 2014;9:221
19. McCarty KS Jr, Miller LS, Cox EB, Konrath J, McCarty KS Sr. Estrogen receptor analyses. Correlation of biochemical and immunohistochemical methods using monoclonal antireceptor antibodies. *Arch Pathol Lab Med* 1985;109:716-721
20. Hwang S, Hong TH, Kim HK, Choi YS, Zo JI, Shim YM, et al. Whole-section landscape analysis of molecular subtypes in curatively resected small cell lung cancer: clinicopathologic features and prognostic significance. *Mod Pathol* 2023;36:100184
21. Wang Y, Jin Y, Shen X, Zheng Q, Xue Q, Chen L, et al. POU2F3: a sensitive and specific diagnostic marker for neuroendocrine-low/negative small cell lung cancer. *Am J Surg Pathol* 2023;47:1059-1066
22. Luan X, Huang Y, Gao S, Sun X, Wang S, Ma L, et al. 18F-alfatide PET/CT may predict short-term outcome of concurrent chemoradiotherapy in patients with advanced non-small cell lung cancer. *Eur J Nucl Med Mol Imaging* 2016;43:2336-2342
23. Osborne JK, Larsen JE, Shields MD, Gonzales JX, Shames DS, Sato M, et al. NeuroD1 regulates survival and migration of neuroendocrine lung carcinomas via signaling molecules TrkB and NCAM. *Proc Natl Acad Sci U S A* 2013;110:6524-6529
24. Osborne JK, Larsen JE, Gonzales JX, Shames DS, Sato M, Wistuba II, et al. NeuroD1 regulation of migration accompanies the differential sensitivity of neuroendocrine carcinomas to TrkB inhibition. *Oncogenesis* 2013;2:e63
25. Cavallaro U, Niedermeyer J, Fuxa M, Christofori G. N-CAM modulates tumour-cell adhesion to matrix by inducing FGF-receptor signalling. *Nat Cell Biol* 2001;3:650-657
26. Khan P, Fatima M, Khan MA, Batra SK, Nasser MW. Emerging role of chemokines in small cell lung cancer: road signs for metastasis, heterogeneity, and immune response. *Semin Cancer Biol* 2022;87:117-126
27. Borromeo MD, Savage TK, Kollipara RK, He M, Augustyn A, Osborne JK, et al. ASCL1 and NEUROD1 reveal heterogeneity in pulmonary neuroendocrine tumors and regulate distinct genetic programs. *Cell Rep* 2016;16:1259-1272
28. Baine MK, Febres-Aldana CA, Chang JC, Jungbluth AA, Sethi S, Antonescu CR, et al. POU2F3 in SCLC: clinicopathologic and genomic analysis with a focus on its diagnostic utility in neuroendocrine-low SCLC. *J Thorac Oncol* 2022;17:1109-1121
29. Hartmann TN, Burger JA, Glodek A, Fujii N, Burger M. CXCR4 chemokine receptor and integrin signaling co-operate in mediating adhesion and chemoresistance in small cell lung cancer (SCLC) cells. *Oncogene* 2005;24:4462-4471
30. Burger M, Glodek A, Hartmann T, Schmitt-Gräff A, Silberstein LE, Fujii N, et al. Functional expression of CXCR4 (CD184) on small-cell lung cancer cells mediates migration, integrin activation, and adhesion to stromal cells. *Oncogene* 2003;22:8093-8101
31. Ma N, Pang H, Shen W, Zhang F, Cui Z, Wang J, et al. Downregulation of CXCR4 by SDF-KDEL in SBC-5 cells inhibits their migration in vitro and organ metastasis in vivo. *Int J Mol Med* 2015;35:425-432
32. Nabet BY, Hamidi H, Lee MC, Banchereau R, Morris S, Adler L, et al. Immune heterogeneity in small-cell lung cancer and vulnerability to immune checkpoint blockade. *Cancer Cell* 2024;42:429-443.e4
33. Dora D, Rivard C, Yu H, Bunn P, Suda K, Ren S, et al. Neuroendocrine subtypes of small cell lung cancer differ in terms of immune microenvironment and checkpoint molecule distribution. *Mol Oncol* 2020;14:1947-1965
34. Tian Y, Li Q, Yang Z, Zhang S, Xu J, Wang Z, et al. Single-cell transcriptomic profiling reveals the tumor heterogeneity of small-cell lung cancer. *Signal Transduct Target Ther* 2022;7:346
35. Kim JT, Li J, Jang ER, Gulhati P, Rychahou PG, Napier DL, et al. Deregulation of Wnt/β-catenin signaling through genetic or epigenetic alterations in human neuroendocrine tumors. *Carcinogenesis* 2013;34:953-961
36. Jin XF, Spoettl G, Maurer J, Nölting S, Auernhammer CJ. Inhibition of Wnt/β-catenin signaling in neuroendocrine tumors in vitro: antitumoral effects. *Cancers (Basel)* 2020;12:345
37. Cives M, Quaresmini D, Rizzo FM, Felici C, D'Oronzo S, Simone V, et al. Osteotropism of neuroendocrine tumors: role of the CXCL12/ CXCR4 pathway in promoting EMT in vitro. *Oncotarget* 2017;8:22534-22549
38. Zhao S, Wang J, Qin C. Blockade of CXCL12/CXCR4 signaling inhibits intrahepatic cholangiocarcinoma progression and metastasis via inactivation of canonical Wnt pathway. *J Exp Clin Cancer Res* 2014;33:103
39. Steele MM, Jaiswal A, Delclaux I, Dryg ID, Murugan D, Femel J, et al. T cell egress via lymphatic vessels is tuned by antigen encounter and limits tumor control. *Nat Immunol* 2023;24:664-675